

# The Diacetone Acrylamide Crosslinking Reaction and Its Control of Core-Shell Polyacrylate Latices at Ambient Temperature

Xinya Zhang, Yanhong Liu, Hong Huang, Yongjin Li, Huanqin Chen

School of Chemistry and Chemical Engineering, South China University of Technology, Guangzhou 510640, China

Received 12 January 2011; accepted 7 April 2011

DOI 10.1002/app.34660

Published online 22 August 2011 in Wiley Online Library (wileyonlinelibrary.com).

**ABSTRACT:** Self crosslinkable core-shell polyacrylate latices (PAs) cured at ambient temperature were synthesized by semicontinuous-seeded emulsion polymerization with diacetone acrylamide (DAAM) and adipic dihydrazide (ADH) as crosslinkable monomers. The influences of DAAM monomer mass content, neutralizer, and curing temperature on the properties of self crosslinkable core-shell latices and the keto-hydrazide crosslinking were discussed. The spectroscopic techniques such as Fourier transform infrared spectroscopy (FTIR), differential scanning calorimeter (DSC), atomic force microscopy (AFM), transmission electron microscopy (TEM), and contact angle instruments were used to determine the structure and properties of PAs. The water evaporating rate during the film-forming process of self crosslinkable core-shell latices was also investigated. FTIR analyses demonstrate that the keto-hydrazide crosslinking reaction does not occur in the latex environment but occurs at ambient

temperature with the evaporation of water during the film-forming process. The results of DSC show that the core-shell crosslinkable PAs have two glass transition temperatures ( $T_g$ ), and  $T_{g,s}$  of crosslinked film are higher than that of non crosslinked film. Moreover, the keto-hydrazide reaction is found to be acid catalyzed and favored by the loss of water and the simultaneous decrease in pH arising from the evaporation of ammonia or amines during film-forming process. Hence, in the volatile ammonia or amines neutralized latices, the latex pH value adjusted to 7–8, which not only ensure the crosslinkable latex with good storage stability but also obtain a coating film with excellent performances by introducing the keto-hydrazine crosslinking reaction. © 2011 Wiley Periodicals, Inc. *J Appl Polym Sci* 123: 1822–1832, 2012

**Key words:** core-shell latex; crosslinking; emulsion polymerization

## INTRODUCTION

The coatings world of today is putting high demands on performance where sustainability, cost, environment, safety, and health aspects are on the priority list of both industry and society.<sup>1–4</sup> Waterborne colloidal polymers (i.e., latices) represent a promising alternative to organic solvent-based systems in coatings applications. Due to the excellent stability and weathering-resistance, water-resistance, alkali-resistance, chemical-resistance, and adhesion properties, polyacrylate latices (PAs) are used in a wide range of coatings.<sup>4</sup> However, the defects of the surface tackiness at high temperature and brittleness at low temperature limited PAs further applications in coatings due to the thermoplastic nature of non crosslinked latices.

To overcome these drawbacks, various crosslinking methods<sup>5</sup> and polymer heterogeneity<sup>6</sup> of latices were

developed. The incorporation of crosslinking chemistry is recognized as a particularly effective means to enhance the mechanical strength, chemical stability, and solvent resistance of the coating film.<sup>7–11</sup> Recently, a system based on the reaction of a carbonyl pendant group on the dispersed polymer backbone with a dihydrazide has been increased interest.<sup>12–18</sup> When dihydrazide is incorporated in the aqueous phase of the latex, this keto-hydrazide reaction offers the most striking advantage of fast, ambient-temperature crosslinking in functionalized PAs. Moreover, to apply the concept of polymer particle heterogeneity is also an effective means to create new and improved materials of polymer latices.<sup>6</sup> For example, by using core-shell particles which have hard domains (formed from a high glass transition temperature ( $T_g$ ) polymer) and soft domains (formed from a low  $T_g$  polymer), it is possible to produce binders with a high block resistance and low minimum film-forming temperature (MFFT).<sup>19,20</sup>

In this article, the crosslinkable core-shell PAs containing diacetone acrylamide (DAAM) [Fig. 1(a)] on the polymer backbone that reacted with an adipic dihydrazide (ADH) difunctional crosslinker [Fig. 1(b)] at ambient temperature were synthesized by a

Correspondence to: X. Zhang (cexyzh@scut.edu.cn).

Contract grant sponsor: National Nature Science Foundation of China; contract grant number: 50803017.

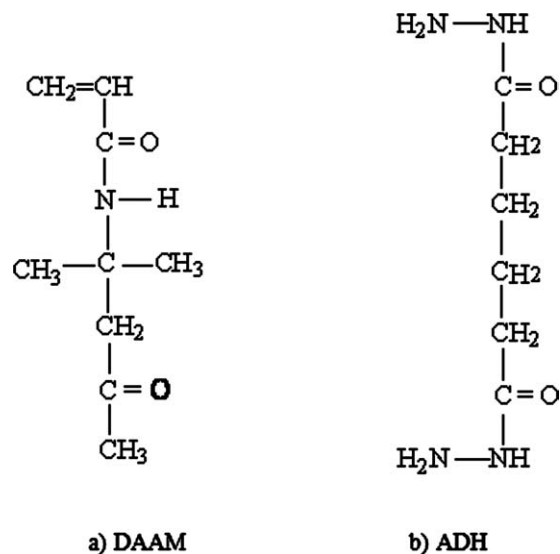


**Figure 1** Chemical structure of diacetone acrylamide and adipic acid dihydrazide.

starve-feed semicontinuous-seeded emulsion polymerization process. It is conceivable that the keto-hydrazide reaction yields hydrazone (Fig. 2).<sup>21</sup> The influences of DAAM monomer on the latex stability, the different neutralizer and the neutralizing degree on the crosslinking reaction were investigated. In addition, the film-forming process of the crosslinkable PAs was also evaluated for controlling the latex

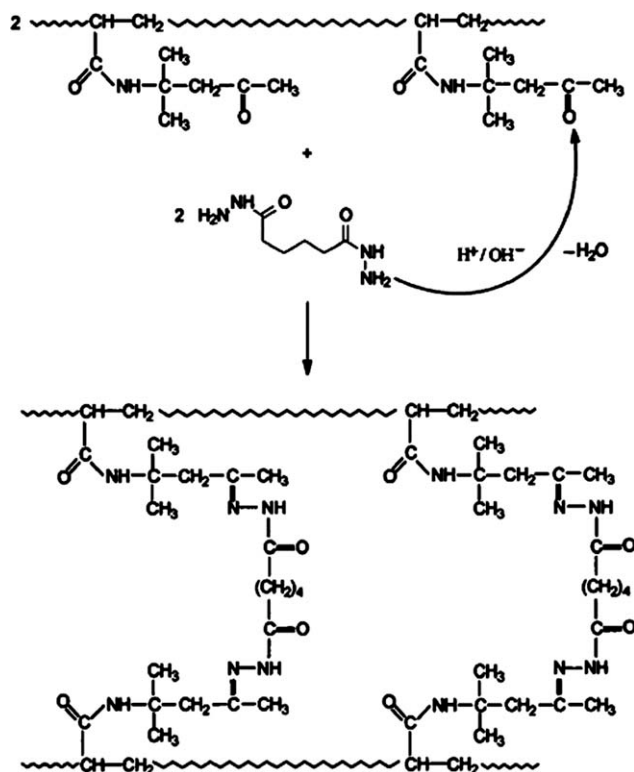


**Figure 2** Schematic diagram of self-crosslinking reaction of DAAM and ADH.

storage stability and the keto-hydrazide reaction development.

## EXPERIMENTAL

### Materials

The monomers *n*-Butyl acrylate (*n*-BA), methyl methacrylate (MMA) and methacrylic acid (MAA), and  $\beta$ -Hydroxypropyl methacrylate ( $\beta$ -HPMA) were purified by reduced pressure distillation (under 300 Pa and 40°C) to remove the inhibitors before used. The crosslinkers diacetone acrylamide (DAAM) and adipic dihydrazide (ADH) were purchased from Aldrich and used as received. The initiator potassium persulfate ( $K_2S_2O_8$ , KPS) was recrystallized before used. The anionic surfactant dodecyl diphenyl ether sodium disulfonate (DSB), nonionic surfactant alkylphenol polyoxyethylene(10) ether (OP-10) (Rhodia), sodium bicarbonate ( $NaHCO_3$ ), and ammonia solution (25%) were of analytical grade and used as received without further purification. Deionized water (DW, self made, specific conductance < 0.057  $\mu$ S/cm) was used for all the purposes. All reactions were carried out in a 1-L flask equipped with a mechanical stirrer (the type of impeller was anchor impeller and the stirring speed was 200 rpm), a condenser, a nitrogen inlet, a thermometer, and a pressure equalizer funnel.

### Synthesis

Synthesis of the crosslinkable core-shell copolymer

The recipe for the synthesis of the core-shell PAs is given in Table I, the theoretical  $T_g$ s of core particles and shell particles are  $-6.22^\circ\text{C}$  and  $42.85^\circ\text{C}$ ,

**TABLE I**  
Recipes for the Core-shell and Random Copolymer Latices

Ingredients	Quantity (g)				
	Crosslinkable core-shell copolymer latex		Core-shell copolymer latex		Random copolymer latex
	core	shell	Core	Shell	
<i>n</i> -BA	49	31	49	31	80
MMA	32	88	32	88	120
MAA	2	2	2	2	4
HPMA	0	4	0	4	4
DAAM	0	2–8	0	0	0
ADH		2–8		0	0
KPS		1		1	1
DSB		2		2	2
OP-10		3		3	3
$NaHCO_3$		1		1	1
DW		220		220	220

respectively. In a typical synthesis, 120 g of water, 1 g of  $\text{NaHCO}_3$ , 2 g of DSB, and 3 g OP-10 were added into the flask and then heated to  $80^\circ\text{C}$  under nitrogen atmosphere. All the core monomer of BA, MMA, and MAA and the shell monomer of BA, MMA, MAA, HPMA, and DAAM were premixed with the predetermined ratio, respectively. When temperature reached  $80^\circ\text{C}$ , 0.25 g of KPS (in 20 mL of water) and 10% of the core monomer mixture were added to the reaction flask in 15 min. Let the reaction run further for 15 min at  $80^\circ\text{C}$ . Then, the rest of core monomer mixture and 0.25 g of KPS (in 40 mL of water) were added through two separate inlets to the flask in 2 h. The temperature was maintained at  $80^\circ\text{C}$ , and the polymerization was carried out for another 30 min. Then, the shell monomer mixture and 0.5 g of KPS (in 40 mL of water) were added to the flask in 2 h. Then, polymerization was carried out for another 1 h. The equimolar ADH was added dropwise. Finally, it was cooled to room temperature and neutralized by ammonia (10%) to get the core-shell particles.

Note that to get a spherical core-shell morphology particle, the ratio of core monomer and shell monomer should be less than 1.<sup>22</sup> By changing the composition of feeding monomers, a series of core-shell crosslinking latex particles were obtained.

#### Synthesis of the noncrosslinkable copolymer and random copolymer

To compare the difference between of the core-shell crosslinkable latex particles, the core-shell non crosslinkable latex particles and the random particles, we prepared the same composition non crosslinkable core-shell and random copolymer latices. The recipes for the non crosslinkable core-shell copolymer and random copolymer are also given in Table I. The preparing process of non crosslinkable core-shell particles is similar to that of the crosslinkable core-shell particles (only without DAAM and ADH added).

For the random copolymer, the theoretical  $T_g$  is  $21.16^\circ\text{C}$ . In a typical synthesis, 120 g of water, 1 g of  $\text{NaHCO}_3$ , 2 g of DSB, and 3 g of OP-10 were added into a 1-L flask and then heated to  $80^\circ\text{C}$  under nitrogen atmosphere. When temperature reached  $80^\circ\text{C}$ , 0.25 g of KPS (in 20 mL of water) and 10% of premixed mixture of all the monomers were added to the system in 15 min. Let the reaction run further for 15 min at  $80^\circ\text{C}$ . Then, all the rest of monomer mixtures and 0.75 g of KPS (in 80 mL of water) were added to the flask in 4 h. The polymerization was continued for another 1 h at  $80^\circ\text{C}$ . Then, it was cooled to room temperature and neutralized by ammonia (10%) to get the random particles.

## Characterization and testing

### Viscosity

The viscosity of PAs was determined by Brookfield Viscometer (Rvdl-II+ with 2 no. rotor) with 60 rpm at  $25^\circ\text{C}$ .

### pH determination

A standard digital pH meter was used with a saturated calomel electrode, and a glass electrode was used to determine the pH value of PAs.

### Crosslinking degree (gel content)

The gel content or insoluble fraction of crosslinked PAs was determined according to ASTM 2765-95a by mass of polymer insoluble after extraction. The sample of about 0.3 g was wrapped in a 120-mesh stainless steel cage and extracted in refluxing xylene containing 1% of antioxidant for 6 h. After extraction, the cage was dried in a vacuum oven at  $55^\circ\text{C}$  until constant weight, the gel content being defined as follows:

Gel content, % = (final weight of sample/initial weight of sample)  $\times$  100 (1)

At least, three samples of each crosslinked polymer were used to yield three values of gel content, the average of which was then reported.

### FTIR analyses

The chemical structure of PAs was analyzed by using a Perkin-Elmer 2000 FTIR Spectrophotometer equipment with a KBr transmission cuvette, the testing range is in  $450\text{--}4000\text{ cm}^{-1}$ .

### DSC analyses

After making the thin coating film, take 5–10 mg of the sheet film sample and place on NETZSCH STA 449C instrument testing at heating rate  $10^\circ\text{C}/\text{min}$  with  $\text{N}_2$  atmosphere.

### Particle size and its distribution analyses

The particle size and its distribution were measured by a Malvern nanoparticle size analyzer (Malvern 2000, British). The latex samples were diluted and dispersed by sonication. The determination of sample concentration is 0.015–0.020%, and the testing range is 0.6 nm to 1  $\mu\text{m}$ .

### AFM analyses

A multimode atomic force microscope (Veeco Dimension 3100, USA) was used to analyze the film surface microphase segregation. The probe is direct

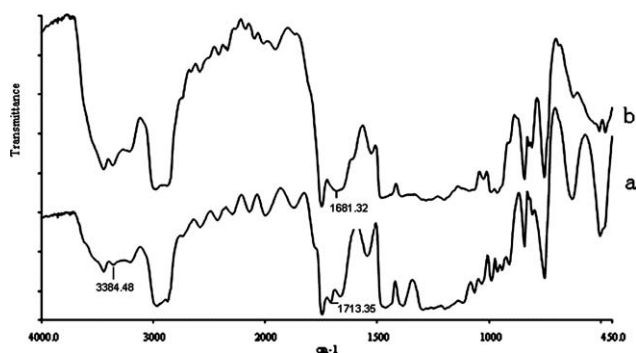


**Figure 3** FTIR spectra of core-shell crosslinkable PA latex and its self-crosslinked latex film.

contacting with the sample surface at room temperature in the air, and the conical probe spring constant of  $\text{Si}_3\text{N}_4$  is 0.06 N/m.

#### TEM analyses

The configuration of the copolymer latex particles was observed by an electric microscope JEM-1010. All the images were taken at a magnification of 20,000 or 100,000. Latex samples were cleaned by using a filtration unit (Advantec MFS Inc. type UPH-76) to remove all water-soluble oligomers and diluted to 3% solids. The diluted latex was treated with 2 wt % aqueous solution of uranyl acetate (UAc). One drop of diluted sample was placed onto copper (Cu) grid and allowed to dry. For potential staining of the shell phase by  $\text{RuO}_4$ , the sample was then exposed to  $\text{RuO}_4$  vapor.

#### Contact angle analyses

A German Dataphysics's OCA20 optical contact angle measuring device was used to measure the surface contact angle of the latex film samples and water.

## RESULTS AND DISCUSSION

#### FTIR analyses

In Figure 3, curve (a) and (b) are the FTIR spectra of the core-shell crosslinkable PA latex and its coating film, respectively, in which DAAM content is 3.0% and equimolar ADH content. The film samples were prepared by the corresponding latices dried at 25°C and relative humidity of 65% for 7 days before measuring. Unless stated otherwise, all the film samples were prepared by the same mode.

From curve (a), there is a strong carbonyl absorption peak at  $1713\text{ cm}^{-1}$ , it belongs to the ketone carbonyl ( $-\text{CH}_2\text{COCH}_3$ ) stretching vibration absorption of DAAM. ADH exhibits a strong band at  $3384\text{ cm}^{-1}$  attributed to the amide carbonyl and N-H stretching. During reaction, it would be expected that the inten-

sity of the ketone carbonyl and the N-H stretching and bending peaks would be weakened, as they are consumed during crosslinking.

From curve (b), all the ketone carbonyl ( $-\text{CH}_2\text{COCH}_3$ ) stretching vibration absorption peak ( $1713\text{ cm}^{-1}$ ) of DAAM and the N-H ( $\text{NH}_2$ ) stretching vibration absorption peak ( $3384\text{ cm}^{-1}$ ) of ADH have disappeared. Comparing the curve (a) and (b), it can be clearly seen that the hydrazone bond ( $\text{C}=\text{N}$ ) characteristic absorption peak presented at the  $1681\text{ cm}^{-1}$  in the curve (b), which is the characteristic of product of the ketone carbonyl and hydrazide crosslinking reaction. It can be deduced that the crosslinking reaction has occurred in the PA film.

#### DSC analyses

DSC is by far the most widely used experimental technique for measuring the thermal properties of thermoset polymers. It has the advantages of simplicity, few limitations, and the capacity to yield simultaneous information regarding kinetics and energetics. Putting 5 to 10 mg non-crosslinked and crosslinked core-shell PA films into the DSC instrument to test their  $T_g$ s, respectively. The testing temperature range was  $-80$  to  $120^\circ\text{C}$ .

In Figure 4, curve (a) is the DSC curve of non-crosslinked PA film, it has two obvious  $T_g$ s,  $-5.1^\circ\text{C}$  belongs to the core polymer and  $45.1^\circ\text{C}$  belongs to the shell polymer. Curve (b) is the DSC curve of self-crosslinked PA film, the  $T_g$ s of core and shell polymers are  $-2.6^\circ\text{C}$  and  $69.0^\circ\text{C}$ , respectively. Compared the curves (a) and (b), it can be found that the  $T_g$  of crosslinked core polymer film is slightly higher than that of the non-crosslinked latex film but the  $T_g$  of shell polymer of self-crosslinked latex film is  $24^\circ\text{C}$  higher than that of the non-crosslinked polymer film. The main reason is that all the DAAM monomer mixed into the shell monomer mixture in the self-crosslinking latex formulation, the ketone carbonyl group of shell polymer reacted with hydrazide during the film-forming process. Thus, the movement of the polymer chain segment was blocked by

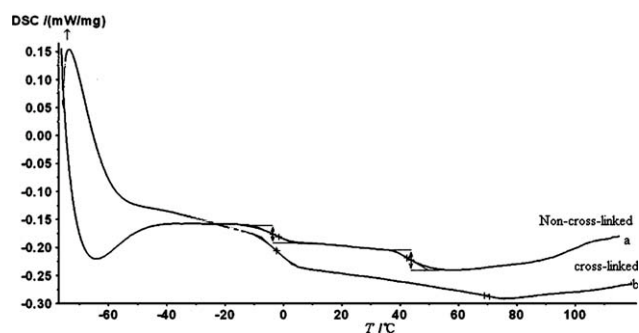


**Figure 4** DSC curves for non-crosslinked and crosslinked core-shell latex films.



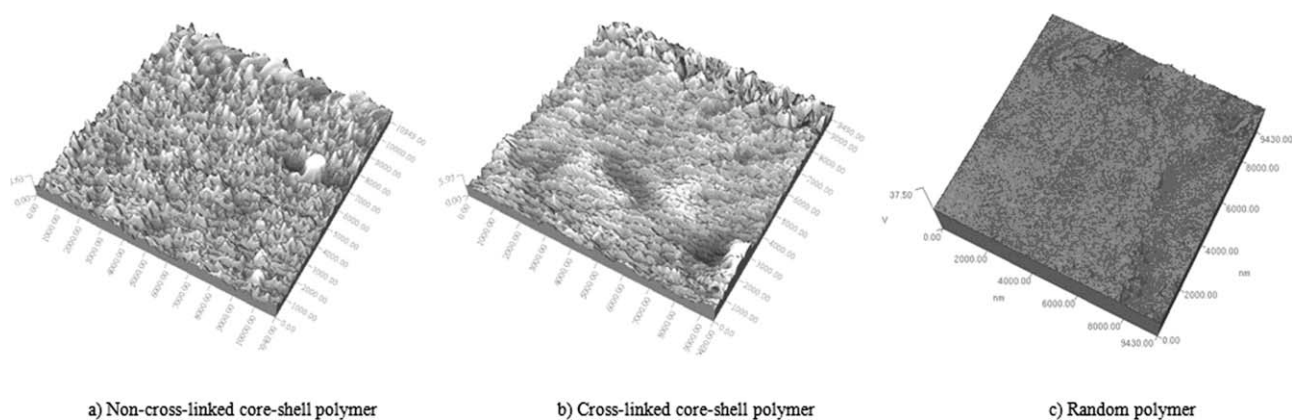


**Figure 5** Three-dimensional AFM images of the core-shell and random PA latex films.

the keto-hydrazide crosslinking reaction, so the  $T_g$  increases significantly and enhances the film's mechanical properties from a macro point of view. On the other hand, due to the keto-hydrazide crosslinking reaction, the  $T_g$  of crosslinked latex film is not as typical as that of linear copolymers. Therefore, the two  $T_g$ s are not obvious in the DSC curve of the crosslinked core-shell PA film in curve (b).

#### AFM analyses

An AFM technique is always used to observe phase and surface structure of polymer. Figure 5(a,b) are the AFM three-dimensional images of the non cross-linked and self crosslinked PA films, and (c) is the AFM image of the random copolymer latex film.

The AFM topographic images of (a) and (b) show that all the film surfaces did not exhibit significant flattening but (c) formed a significant flatter film. There are both some convex and concave parts presented on the surfaces of the core-shell PA films. In this case, the roughness is caused by microphase

segregation of the core-shell particles. The part of dark color and distributed in the "trough" is the soft segment of thermoplastic PAs, which is the continuous phase distribution. While the hard segment is the light color and upper part due to the high surface energy and formed the dispersed phase.<sup>23,24</sup> Comparing through the images (a) and (b), the surface of crosslinked PAs is smoother than that of non crosslinked polymer. It may be that the denser and smoother coating film was achieved due to the keto-hydrazine crosslinking reaction occurred. For random copolymer, because there is not microphase segregation presented, so the surface formed a significant flatter film in image (c).

#### TEM analyses

TEM micrographs of the core-shell particles and the same composition random copolymer particles are shown in Figure 6. All these micrographs show that both core-shell particles as well as random copolymer particles are spherical, and both particle

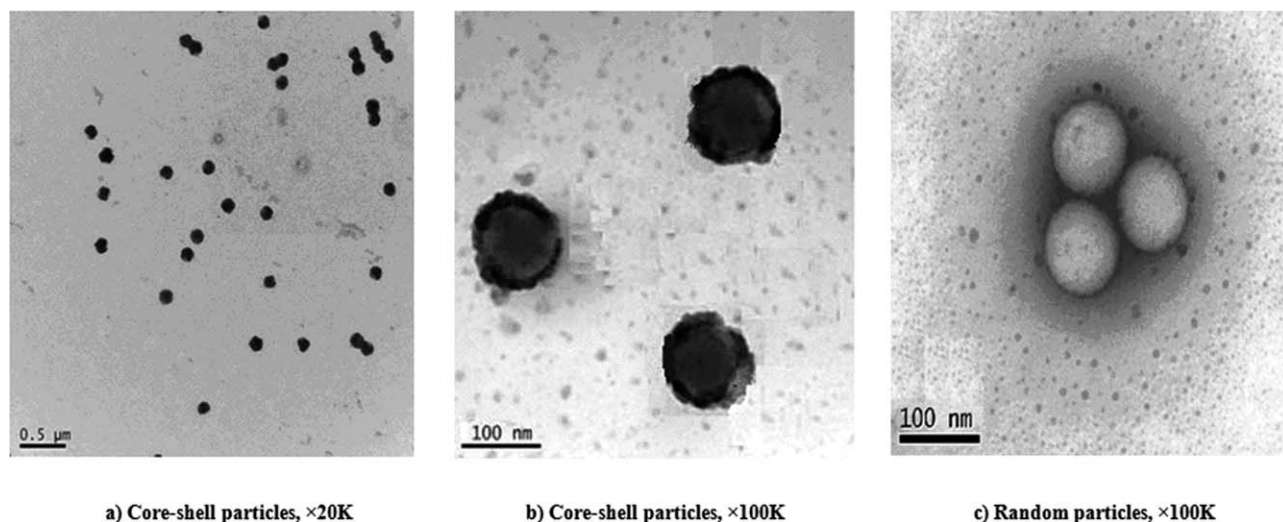


**Figure 6** TEM photographs of the crosslinkable core-shell and random polymer latex.

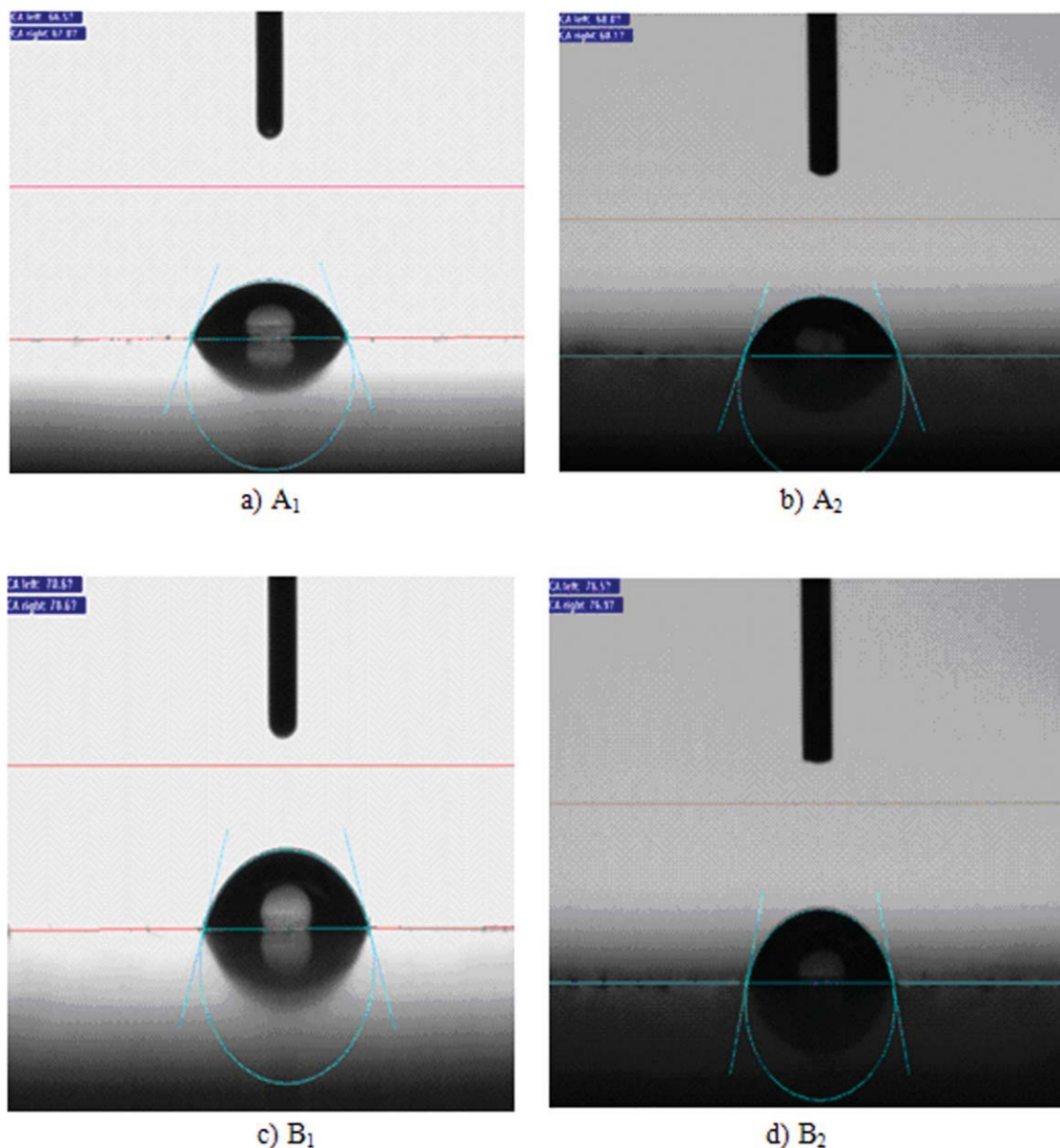


**Figure 7** Contact angles of non crosslinked and crosslinked PA films with water. [Color figure can be viewed in the online issue, which is available at [wileyonlinelibrary.com](http://wileyonlinelibrary.com).]

sizes are of almost  $0.1 \mu\text{m}$  in diameter. It indicates that there are no new particles generated during the semicontinuous-seeded emulsion polymerization and the particle size distributions are uniform.

To further observe the core-shell particles morphology, some part of anywhere of Figure 6(a) was enlarged as shown in Figure 6(b). Figure 6(b) shows clearly a slight difference in contrast between the outer and inner portion of the particles. The light gray inner portion of the latex particle is the core layer, and the dark outer layer is shell polymer, which indicates the shell monomers are reacted on the core particle surface. The clear phase separation between the core and shell phases leads to a well-defined core-shell morphology.<sup>25</sup>

### Contact angle analyses

The contact angles of the non crosslinked and crosslinked PA film samples with water are shown in Figure 7, wherein  $A_1$  is the non crosslinked PA film after dried 3 days,  $A_2$  is the non crosslinked PA film after dried 7 days,  $B_1$  is the crosslinked PA film after dried 3 days, and  $B_2$  is the crosslinked PA film after dried 7 days. The contact angles of  $A_1$  and  $A_2$  are  $66.5^\circ$  and  $68.0^\circ$ , respectively. The contact angles of  $B_1$  and  $B_2$  are  $70.6^\circ$  and  $76.5^\circ$  under the same conditions. Due to the smoother and denser network structure of coating film formed by keto-hydrazine crosslinking reaction that creates a three-dimensional network, water molecules cannot easily penetrate and

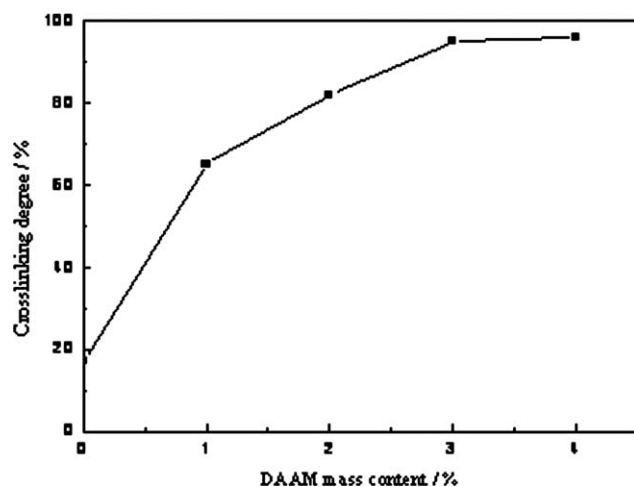


**Figure 8** Effects of DAAM mass content on crosslinking degree.

thus the contact angle becomes larger. In addition, the contact angle of self crosslinked PA film with water increased more than that of the non crosslinked latex film with the increasing drying time. It indicates that the excellent water resistance is another remarkable character of the crosslinked latex film.

#### Effect of DAAM content on the keto-hydrazide crosslinking degree

Degree of crosslinking is a main factor controlling properties of the crosslinked products. The approach, which is widely used in the determination of crosslinking degree, is based on ASTM 2765-95a.<sup>26,27</sup> The method involves measuring the content of gel or the insoluble fraction produced in the crosslinked material after extracting with solvents. In this article, the gel content or insoluble fraction of crosslinked PAs was determined according to ASTM 2765-95a by mass of polymer insoluble after extraction.

DAAM content in carboxyl-functional polymer latex has an impact on the crosslinking degree, but DAAM mass content is limited to below 5.0% to maintain its original performance during storage time.<sup>5</sup> The crosslinkable PAs with different DAAM content of 1.0%, 2.0%, 3.0%, and 4.0% were prepared, respectively. The results of different DAAM mass content on crosslinking degree are shown in Figure 8.

It can be seen from Figure 8, even though the mass fraction of DAAM is 0, there is still a certain content of gel after the coating film was extracted with xylene. This is due to the copolymerization effect of carboxyl and hydroxyl functional monomers on the core polymer. On the other hand, some branching and crosslinking between molecules may also occur due to the active chain transfer to polymer molecules during the polymerization process. It can be seen the crosslinking degree is close to 95% when the mass fraction of DAAM is 3%. The crosslinking degree does not increase significantly with the further increasing of DAAM mass content. The resulted crosslinking structure from the keto-hydrazide reaction prevents water component from evaporating during the film-forming process. In the same time, it also inhibits the molecular chain diffusion and further hindered the progression of the crosslinking reaction. This is another reason why the DAAM mass content was limited to below 5.0% in the crosslinkable copolymer latices.

#### Effect of pH value on the crosslinkable PAs properties

Determination of the crosslinking reaction condition

For the self crosslinkable latex cured at room temperature, the crosslinking reaction rate and the crosslinking degree have great impact on the film properties. The keto-hydrazine reaction is a dehydration reaction, and the reaction is inhibited by the presence of water. Therefore, the keto-hydrazide crosslinking in a latex film is not expected to occur unless sufficient fraction of the water component has evaporated. The literature indicates that the keto-hydrazide crosslinking reaction is often catalytic affected by the latex pH value.<sup>28</sup> A serial of experiments of the keto-hydrazide crosslinking reaction conditions were designed to address pH evolution during film formation and determine when the crosslinking reaction developed. Dissolving 10 g of DAAM and 10 g of ADH in 50 mL pH value of 8 dilute sodium hydroxide solution, 50 mL deionized water (pH = 7.0), and 50 mL pH value of 6, 5, and 4 dilute hydrochloric acid solution, respectively, with stirring at room temperature, then observe whether and when the deposition in solution generated. The experimental results are shown in Table II.

**TABLE II**  
Influence of the Latex pH Value on the Keto-hydrazide Crosslinking Reaction

pH	8	7	6	5	4
Phenomena	No deposition after 48 h	No deposition after 48 h	Muddy and deposition after 5 h	Muddy and deposition after 1.5 h	Muddy and deposition after 0.5 h
Storage shift (month)	11	8	3	<1	<1



**TABLE III**  
Storage Stability of the Crosslinkable PA Latex

No.	A	B	C	D
Color change	Some darker	Some darker	Darker	Darker
Viscosity change	No	Little	Little	Little
Deposition	No	No	No	No
Particle size (nm)	98.6	97.8	98.5	98.9

DAAM and ADH coexist stably in the neutral or basic environment, but the keto-hydrazide crosslinking reaction occurs at once in the solution even if the system was weak acidity. The crosslinking reaction rate is increasing significantly with the decreasing pH value. The results indicate that the ADH is partitioned mainly in the aqueous phase initially and can enter into the polymer phase during the later stages of film formation.

On the other hand, the crosslinkable PA latex storage shift decreases with the decreasing pH value from Table II. Because the condensation polymerization of ketone carbonyl and hydrazide needs catalyzing by weak acidity, the reactivity of carbonyl can be enhanced by the combination of carbonyl and protons. During the storage period or the first cured stage, the carboxylic acid presented as carboxylic amine salt form, the latex system is neutral, and the carboxylic acid does not act as a catalyst. During the continuous curing process, the pH value decreases and the crosslinking reaction can be enhanced by the catalytic role of carboxylic acid with the ammonia volatilizing. Therefore, to prevent DAAM and ADH react prematurely in the latex system, the latex pH value should be adjusted to neutral or alkaline after the completion of the emulsion polymerization before ADH added dropwise into the latex system.

#### Storage stability of the crosslinkable PAs

The latex pH value is a key factor affecting the self-crosslinkable latex storage stability. The keto-hydrazide crosslinking reaction belongs to the post-crosslinking system. The prerequisite condition is that ketone carbonyl does not react with hydrazine during the storage period. The crosslinkable polymer latex properties such as particle size and viscosity would change if the crosslinking reaction occurs during the storage period. To investigate the crosslinkable PAs storage stability, the PAs with DAAM content of 3.0% and all DAAM mixed into the shell monomers were prepared, and the pH value was adjusted to 7 by using ammonia before a equimolar ADH added. The results of the above self-crosslinkable PAs placed at 60°C (for accelerated test) for 2 weeks (named as A), 4 weeks (named as B), 6 weeks (named as C), and 8 weeks (named as D) are shown in Table III, respectively.

As can be seen from Table III, there is no deposition, little change in viscosity and particle size of the self-crosslinking PAs after storage for 2, 4, 6, and 8 weeks at 60°C, respectively. It indicates that the self-crosslinking PAs have good storage stability and the keto-hydrazide crosslinking reaction does not occur in the latex environment during the latex storage period.

#### Effect of neutralizer on the keto-hydrazide crosslinking degree

The effect of different neutralizers on the crosslinking degree was also investigated for the self-crosslinkable PAs with DAAM content of 3.0%. The results of crosslinking degree tested every 24 h are shown in Figure 9. With the evaporating of water during the film-forming process, the volatile neutralizer is also evaporating with water, so the latex system becomes acidic from basic gradually and induces the keto-hydrazide crosslinking reaction to occur. The crosslinking degree was observed to increase sharply with an increasing of crosslinking time. The slope of the graph is very steep in the early stage of crosslinking, inferring a high crosslinking rate in this stage.

The crosslinking reaction rate becomes faster and the keto-hydrazide crosslinking degree increases faster when the neutralizer evaporates faster. When ammonia used as the neutralizer, the increasing rate of crosslinking degree is the fastest, it means that the fastest crosslinking reaction rate is achieved. Then, it follows by the ethylamine, diethylamine, ethylenediamine, and triethylamine. Nonetheless, when sodium hydroxide used as neutralizer, the increasing rate of crosslinking degree and the final crosslinking degree are far lower than that of ammonia and the other volatile organic neutralizers. This is also further verifying that the crosslinking reaction

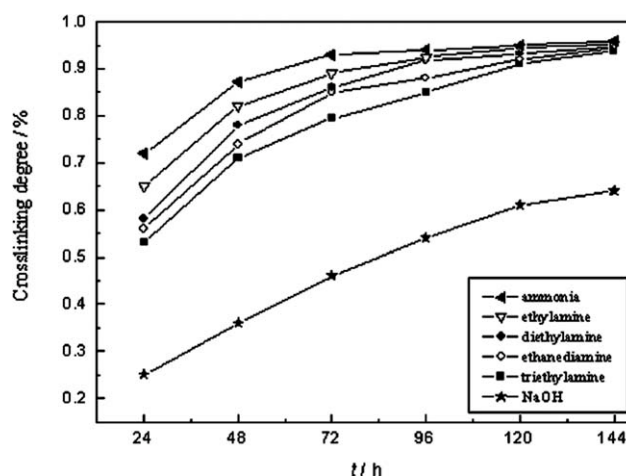


**Figure 9** Effects of different neutralizers on crosslinking degree.



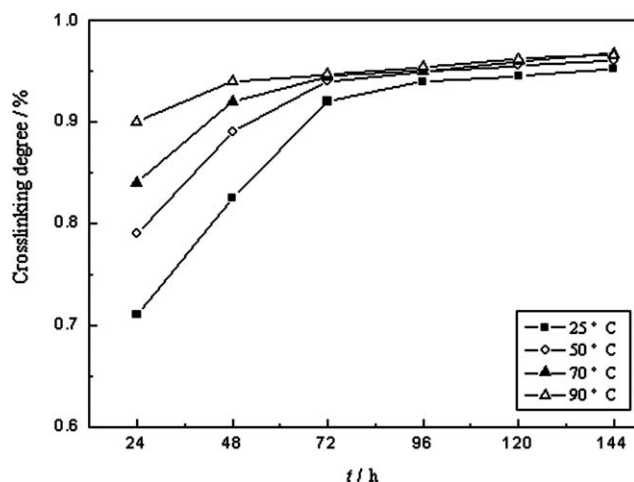


**Figure 10** Effects of cured temperature on crosslinking degree during the film forming process.

occurs only under acid-catalyzed condition in the volatile amine system.

#### Effect of cured temperature on the keto-hydrazide crosslinking degree

Although the keto-hydrazide crosslinkable PAs can cure at room temperature, it need very long time to reach its maximum crosslinking degree. Generally speaking, the faster crosslinking rate is obtained with the higher curing temperature for the crosslinkable PAs. In this serial experiment, the crosslinking degrees of PAs with DAAM content of 3.0% and DAAM all mixed into the shell monomers were tested every 24 h under the cured temperature of 25°C, 50°C, 70°C, and 90°C, respectively. The results are shown in Figure 10.

From Figure 10, the time for achieving the maximum crosslinking degree decreases obviously with the higher cured temperature. At room temperature, the crosslinking reaction needs 7 days to complete, and reaches the final crosslinking degree of 95%. At 50°C and 70°C, the time of crosslinking reaction is about 48 h. When the cured temperature reached 90°C, the time to finish the crosslinking reaction is only 24 h. On the one hand, ADH in aqueous phase diffuses faster with the higher cured temperature, so the time of ADH to contact with the latex particle surface becomes shorter. Instantaneously, the evaporating of water molecules becomes faster and so does the crosslinking reaction rate. On the other hand, the latex particles are taking on different states at different temperatures. The higher cured temperature can make latex particles take on high-elastic state, and even viscous flowing state, which contributes to the proliferation of fusion particles, and reduces the gaps and deficiencies of the coating films. So the degree of mutual integration between

polymer particles enhances with the higher cured temperature, thus the crosslinked coating film becomes denser and smoother with the increasing crosslinking degree.

In addition, the final crosslinking degree is 95% at room temperature, and the final crosslinking degrees under different higher cured temperatures have not obvious changes. It indicates that the self crosslinking reaction of the core-shell PAs have finished after dried 7 days at room temperature.

#### Film-forming process of the self crosslinking core-shell PAs

The dispersion of crosslinkable latex-type film-forming materials is water. In waterborne systems, the time at which crosslinking occurred in the film formation process has a profound effect on the properties.<sup>8,11,29-33</sup> To achieve maximum film strength, particles should remain relatively free of crosslinking in the dispersion but undergo extensive crosslinking once they have formed a coating film on the substrate. The evaporating of water from crosslinkable latex is an important factor to determine the changes in viscosity of the wet latex film. Due to the water evaporating rate is much slower than general organic solvents, it makes the viscosity of the wet latex film increase too slowly and easy to sag, thus the latex-based applications are subjected to certain restrictions.

The water evaporating from the latex system is a very complex process, and it is always affected not only by some factors such as temperature, humidity, and airflow and so on, but also by the interaction between the film-forming polymer latex and dispersion. Even it may be impacted by the diffusing velocity of water from the inner to the film surface after the wet film lost its mobility. Figure 11 shows

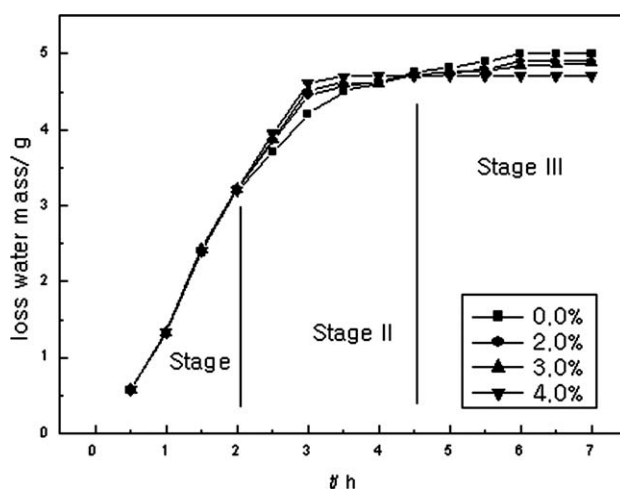


**Figure 11** Film-forming processes of PAs with different DAAM mass content.

the film-forming process of PAs with different DAAM mass contents under the surrounding of 25°C and relative humidity of 65%.

In Figure 11, the water mass loss curves can be divided into three stages. The initial stage (Stage I) is the free water evaporating stage, where the evaporating mass of water increases linearly with time. The water evaporating rate keeps constant during this stage.<sup>2</sup> In the Stage II, the water evaporating rate begins to decline, this is due to the water in the latex surface cannot be supplemented, and the water/air interface decreases. In this stage, the surface tension (capillary force) of this latex begins to play a major role in affecting the water evaporation.<sup>34</sup> For Stage III, the majority of moisture has volatilized, the continuous film is formed on the surface of latex. The water evaporating rate only depends on the diffusing capacity of the residual water in wet film through the gaps between particles and the polymer film, so does a further decline of loss rate.<sup>35</sup>

For the crosslinkable PAs contained DAAM, the surface tension is less than that of the non crosslinked PAs, its internal molecules are more accessible to the surface layer and more helpful for the surface water molecules evaporating. Therefore, in Stage II, the particle size is smaller if the higher content DAAM presented in the latex system, and its whole surface area becomes larger, so the faster rate of water evaporating is achieved. However, with the DAAM content further increases, the crosslinking degree further increases, the formed network structure by crosslinking hinders the further proliferation of water molecules. So in Stage III, the moisture evaporating rate actually slows down with the higher DAAM level.

Based on the above analyses, the three stages of film-forming process are named as the filling of latex particles, the crosslinking reaction, and the proliferation. In Stage I, the original latex particles stabilized by the electrostatic repulsion and steric effects become stronger with the water evaporation. The original latex particles are still free to move. The water evaporating rate is about equal to the evaporating rate of pure water and the evaporating rate is the same as free water evaporation. In Stage II, with the further evaporating of water, the latex particles are irreversible mutual contacted and the neutralizing reaction carries out simultaneously. The produced alkali neutralizer volatilizes out; therefore, the latex system becomes acidic from basic. A network polymer chain has formed by the crosslinking of ADH and DAAM in the shell monomers. The latex particles integrate together with each other through ADH and particle deforming, and then stack to form a denser state. In Stage III, the polymer molecular chain is interdiffusing, penetrating, winding, and then forming a film with certain mechanical properties by shrinking force or surface tension.<sup>36</sup>

## CONCLUSIONS

With MMA, BA as the main comonomers, DAAM and ADH as crosslinkers, semicontinuous-seeded emulsion polymerization was carried out to prepare self crosslinking PAs. The prepared PAs at room temperature with the core-shell structure were by ADH postadded. The FTIR spectroscopy results show that the keto-hydrazide crosslinking reaction does not occur under alkaline condition in the latex environment but occurs during the film-forming process with the evaporation of water at ambient temperature. DSC analyses demonstrate there are two  $T_g$ s in PAs with core-shell structure, and the keto-hydrazide crosslinking reaction enhancing the crosslinkable copolymer's  $T_g$ .

The main factors such as DAAM mass content, the latex pH value, different types of neutralizers, and cured temperature have significant impacts on the keto-hydrazide crosslinking reaction. Moreover, the keto-hydrazide crosslinking reaction is acid catalyzed and the crosslinking reaction is favored by the loss of water and the simultaneous decrease in pH arising from the evaporation of ammonia or amines during film-forming process. Hence, in the volatile ammonia or amines neutralized latices, the latex pH value was adjusted to 7–8, which not only ensure the crosslinkable latex storage stability, but also get a coating film with excellent performances by introducing the keto-hydrazine crosslinking reaction that creates a three-dimensional network.

## References

1. Kerhsaw, Y. *Eur Coat J* 1998, 4, 230.
2. Steward, P. A.; Hearn, J.; Wilkinson, M. C. *Adv Colloid Interface Sci* 2000, 86, 195.
3. Provdar, T.; Urban, M. W. *ACS Symposium Series*, American Chemical Society: Washington DC, 790; Oxford University Press: vii 2001.
4. Keddie, J. L. *Mater Sci Eng Rep* 1997, R21, 3.
5. Yasuharu, N. *Prog Org Coat* 2004, 51, 280.
6. Overbeek, A. *J Coat Technol Res* 2010, 7, 1.
7. Hellgren, A. C.; Wallin, M.; Weissenborn, P. K.; McDonald, P. J.; Glover, P. M.; Keddie, J. L. *Prog Org Coat* 2001, 43, 85.
8. Aradian, A.; Raphael, E.; De Gennes, P. G. *Macromolecules* 2000, 33, 9444.
9. Buckmann, F.; Overbeek, A.; Nabuurs, T. *Eur Coat J* 2001, 6, 53.
10. Pinenq, P.; Winnik, M. A. *J Coat Technol* 2000, 72, 45.
11. Winnik, M. A. *J Coat Technol* 2002, 74, 49.
12. Bakker, P.; Mestach, D. *Surf Coat Int B: Coat Trans* 2001, 84, 243.
13. Lee, S. B.; Billiani, J.; Pfohl, W. F.; Lee, K. I. *Proceedings of 30th International Waterborne, High Solids and Powder Coatings Symposium*; New Orleans, 2003.
14. Hanrahan, B.; Hakko, K.; Murayama, T.; Hotta, I. *FSCT Mid-year Symposium: Crosslinking for Coatings—Meeting the Challenges*; Orlando, 2004.
15. Esser, R. J.; Devona, J. E.; Setzke, D. E.; Wagemans, L. *Prog Org Coat* 1999, 36, 45.
16. Mestach, D. *FATIPEC Congress 25th 2000*, 2, 347.

17. Mestach, D.; Ahmed, M. Proceedings of 28th International Waterborne, High Solids and Powder Coatings Symposium; 2001; p 195.
18. Fischer, G. C.; Fioravanti, L. C.; Frazza, M. S. Rohm and Haas Company, U.S. Pat.US006,512,042B1 (2003).
19. Schuler, B.; Baumstark, R.; Krisch, S.; Pfau, A.; Sanor, M.; Zosel, A. Prog Org Coat 2000, 40, 139.
20. Borthakur, L. J.; Dolui, T.; Jana, S. K. J Coat Technol Res 2010, 7, 765.
21. Yasuharu, N. Prog Org Coat 1997, 31, 105.
22. Zhang, X. Y.; Sun, Z. J.; Fu, H. Q.; Huang, H.; Lan, R. H.; Chen, H. Q. J Natur Sci Hunan Norm Univ 2006, 29, 62.
23. Tang, Y. W.; Labow, R. S.; Revenko, I.; Santerre, J. P. J Biomater Sci Polym Ed 2002, 13, 463.
24. Li, L. M.; Huang, X. A. J Donghua Univ (Natur Sci) 2004, 3, 9.
25. Cho, I.; Lee, K. J Appl Polym Sci 1985, 30, 1903.
26. Kalyanee, S.; Darinya, M. J Appl Polym Sci 2004, 93, 901.
27. Shieh, Y. T.; Liao, J. S.; Chen, T. K. J Appl Polym Sci 2001, 81, 186.
28. Nicola, K.; Illsley, D. R.; Keddie, J. L. J Coat Technol Res 2008, 5, 285.
29. Winnik, M. A. Polym Prepr 2003, 44, 100.
30. Tronc, F.; Liu, R.; Winnik, M. A.; Eckersley, S. T.; Rose, G. D.; Weishuhn, J. M.; Meunier, D. M. J Polym Sci Part A: Polym Chem 2000, 40, 2609.
31. Tamai, T.; Pinenq, P.; Winnik, M. A. Macromolecules 1999, 32, 6102.
32. Brown, W. T. J Coat Technol 2000, 72, 63.
33. Taylor, J. W.; Winnik, M. A. J Coat Technol Res 2004, 1, 163.
34. Tirumkudulu, M. S.; Russel, W. B. Langmuir 2004, 20, 2947.
35. Vanderhoff, J. W.; Bradford, E. B.; Carrington, W. K. J Polym Sci Polym Symp 1973, 41, 155.
36. Winnik, M. A. Curr Opin Colloid Interface Sci 1997, 2, 192.